Preferred orientation of experimentally deformed Mt Isa chalcopyrite ore

E. M. JANSEN, H. SIEMES

Institut für Mineralogie und Lagerstättenlehre, RWTH Aachen, 5100 Aachen, Germany

P. MERZ, W. SCHÄFER, G. WILL

Mineralogisches Institut, Universität Bonn, Außenstelle Forschungszentrum Jülich (KFA), 5170 Jülich, Germany

AND

M. DAHMS

Forschungszentrum Geesthacht (GKSS), Max-Planck-Straße, 2054 Geesthacht, Germany

Abstract

Chalcopyrite samples from Mt Isa, Australia have been experimentally shortened by up to 30% at temperatures up to 450 °C, at a constant confining pressure of 300 (400) MPa, and different strain rates in the range from 10^{-5} to 10^{-8} sec^{-1}. After deformation, the X-ray pole figures show a maximum of (220/204) perpendicular to the compression axis for each of the samples, which has already been described for room temperature experiments by Lang (1968). The overlapping pseudocubic peaks of chalcopyrite can be separated into true tetragonal peaks by neutron diffraction texture analysis using a position sensitive detector combined with profile analysis (Will *et al.*, 1989). The five investigated samples each show a combination of two or four main orientations of the crystallites, which represent neither a pseudocubic nor a tetragonal fibre texture.

KEYWORDS: chalcopyrite, experimental deformation, preferred orientation, X-ray texture analysis, neutron diffraction texture analysis.

Introduction

A LOT of work has been done on the experimental deformation of polycrystalline chalcopyrite since the early studies of Mügge (1920). The most recent experiments performed under well-defined deformation conditions are those of Atkinson (1974), Kelly and Clark (1975) and Roscoe (1975). However, investigations of preferred orientation of chalcopyrite after deformation have only been performed by Lang (1968), and then only for room temperature experiments. Lang found a maximum of the (220/204) double reflection perpendicular to the compression axis which became stronger with increasing strain. The chalcopyrite reflections can only be measured as pseudocubic reflections in X-ray texture goniometry, because of the chalcopyrite structure, a tetragonal derivative of the cubic sphalerite structure with a ratio of $c_0/a_0 = 1.97$. Lang (1968) interpreted the chalcopyrite preferred orientation as a (220/204) fibre texture similar to the cubic (220) fibre texture of sphalerite. Axial deformation leads to a fibre texture, which is an axial preferred orientation with a crystallographic direction parallel to the compression axis. In the centre of the pole figure of a lattice plane perpendicular to this direction, a circular maximum can be found. All other lattice planes have continuous pole density distributions on circles around the centre of the pole figures. In the incomplete (220/204) chalcopyrite X-ray pole figures, Lang (1968) found a central maximum and a circular distribution at a pole distance of 60°, which corresponds to a cubic (220) fibre texture. The (112) pole figures, corresponding to the cubic (111), showed a small circle distribution at about 36° off the centre of the projection. However, even in the pole figures with high intensities the fibres have not developed perfectly. If undeformed specimens are inhomogeneous or have a preferred orientation initially, then the final pole density of the circles deviates from perfect axial symmetry. Cubic deformation

Mineralogical Magazine, March 1993, Vol. 57, pp. 45–53

mechanisms have generally been assumed for chalcopyrite (Mügge, 1920; Lang, 1968; Kelly and Clark, 1975; Roscoe, 1975). However, X-ray, optical and TEM studies of chalcopyrite single crystals have shown that several real tetragonal slip and twinning modes are activated in deformation experiments (Couderc and Hennig-Michaeli, 1988). The aim of the present investigation was to control the development of preferred orientation under different experimental conditions, and to try to measure real tetragonal reflections by means of neutron diffraction texture analysis.

Starting material and experimental conditions

For the deformation experiments, cylindrical samples of 30 mm length and 15 mm diameter were prepared from Mt Isa material with an average composition of 85.4 ± 5.0% chalcopyrite, 2.9 ± 1.7% pyrrhotite, 1.1 ± 2.0% pyrite, and 10.6 ± 4.5% quartz and other minerals. The grain diameters in the samples varied from 10 μm to 1.5 mm, the average being 300 μm. The samples were deformed by axial compression with 300 MPa confining pressure at temperatures from 100 to 450 °C, and 400 MPa confining pressure at room temperature. For the 21 experiments several strain rates were applied in the range from 10^{-5} to 10^{-8} sec^{-1}. Because of the rather short experimental length, 13 experiments were conducted with a strain rate of 3×10^{-5} sec^{-1}. Most experiments were stopped after about 10–15% shortening, some after about 25–30%. Table 1 gives the experimental conditions for all samples.

Measurement of preferred orientation

For X-ray texture analysis, performed with a Siemens texture goniometer in reflection mode (Cr–$K\alpha$, 30 kV, 16 mA), slices of 2 mm thickness were cut perpendicular to the long axis of each cylinder. For the measurement of undeformed samples, slices were also cut from both ends of the cylinders, where possible, before preparing them to exactly 30 mm length. Only the (112) and (220/204) reflections of chalcopyrite can be measured by X-ray texture goniometry, all other reflections

Table 1. Experimental Conditions

Sample No.	Temperature (°C)	Strain rate (sec^{-1})	Total strain (%)	Exp. length	Stress diff. at 10% strain (MPa)
CH8505	25	2.2×10^{-5}	9.30	1.5h	
CH8218	25	2.4×10^{-5}	24.82	3.1h	869
CH8503	100	2.6×10^{-5}	11.76	1.5h	775
CH8319	100	2.6×10^{-5}	26.71	3.1h	737
CH8504	200	2.7×10^{-5}	12.63	1.5h	663
CH8409	200	2.7×10^{-5}	28.38	3.2h	560
CH8301	200	6.4×10^{-6}	13.81	6.2h	460
CH8507	200	2.8×10^{-6}	13.73	15.5h	424
CH8404	200	2.8×10^{-7}	13.70	6.1d	323
CH8509	250	2.6×10^{-5}	13.98	1.7h	414
CH8506	300	2.8×10^{-5}	14.39	1.5h	357
CH8510	300	2.8×10^{-5}	30.22	3.1h	318
CH8508	300	2.9×10^{-6}	14.98	15.0h	256
CH8402	300	2.9×10^{-7}	15.41	6.2d	173
CH8411	400	2.8×10^{-5}	15.75	1.6h	157
CH8410	400	2.8×10^{-5}	31.59	3.1h	193
CH8308	400	2.9×10^{-6}	15.43	15.4h	124
CH8303	400	3.0×10^{-7}	15.62	6.1d	164
CH8408	400	6.0×10^{-8}	15.10	29.2d	87
CH8309	450	2.8×10^{-5}	15.88	1.6h	145
CH8304	450	2.9×10^{-5}	21.56	2.2h	140

are too weak. For neutron texture analysis, half of the deformed cylinders were used. Five samples were investigated with neutron diffraction at the KFA Jülich, using a position sensitive detector combined with profile analysis (Will *et al.*, 1989). Thus, a large number of chalcopyrite reflections could be measured simultaneously and the double reflections could be separated into true tetragonal reflections. The complete pole figures of the following reflections were used for the interpretation: (112), (200), (004), (220), (204), (312), (116), (224), (400) and (008). The series of pole figures for each sample were also used to calculate orientation distribution functions (ODFs) by means of the iterative series expansion method using the positivity condition (Dahms and Bunge, 1989*a*,*b*; Dahms, 1992). The ODFs are presented in sigma sections (Matthies *et al.*, 1990). Each section contains the density distribution for all crystal orientations with a constant ($2\sigma = (\alpha + \gamma)$ in dependence on azimuth α and pole distance β, (where α, β and γ are the Euler angles of an orientation). An arbitrary point (α,β) within a sigma section gives the direction of the <001>-crystal axis of that orientation with reference to the specimen axes. 2σ gives the rotation around the *c*-axis. The average distribution of all sigma sections is identical to the (001) pole figure. From the ODFs the pole figures were recalculated.

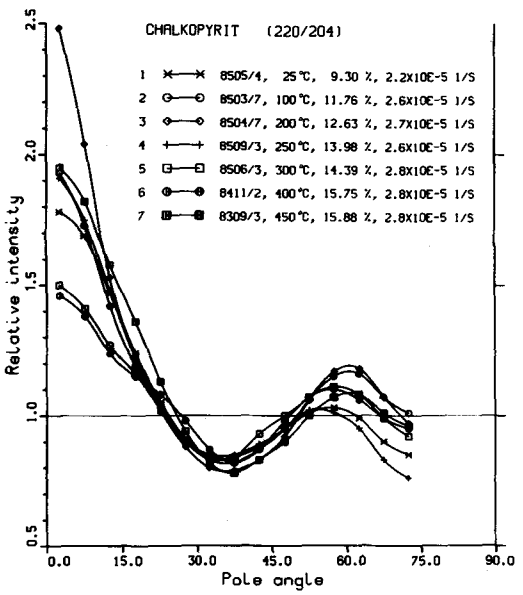

FIG. 2. (220/204) X-ray fibre textures (in averaged density profiles) of Mt Isa chalcopyrite shortened by up to 16 per cent, at a constant strain rate of about 3×10^{-5} sec^{-1}, and different temperatures as indicated on the diagram.

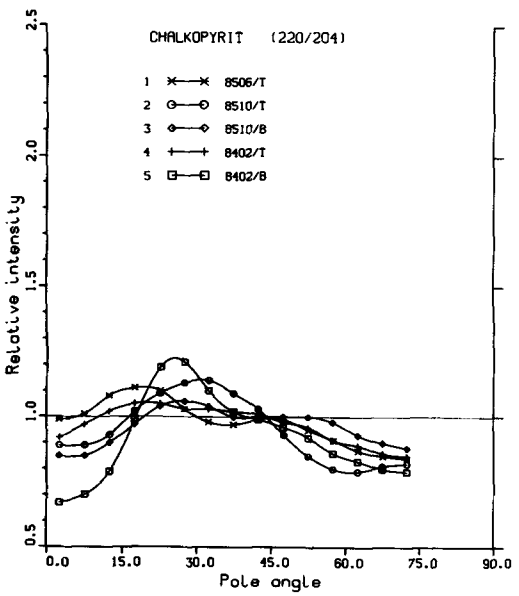

FIG. 1. Representative examples showing X-ray measured preferred orientation of undeformed Mt Isa chalcopyrite (averaged density profiles).

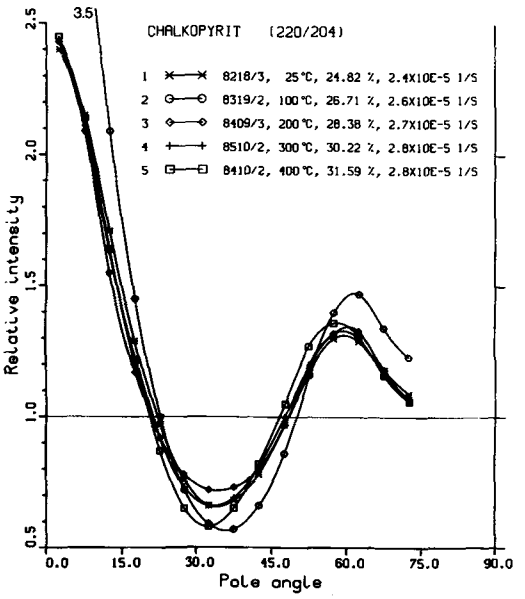

FIG. 3. (220/204) X-ray fibre textures (in averaged density profiles) of Mt Isa chalcopyrite shortened by up to 32 per cent, at a constant strain rate of about 3×10^{-5} sec^{-1}, and different temperatures as indicated on the diagram.

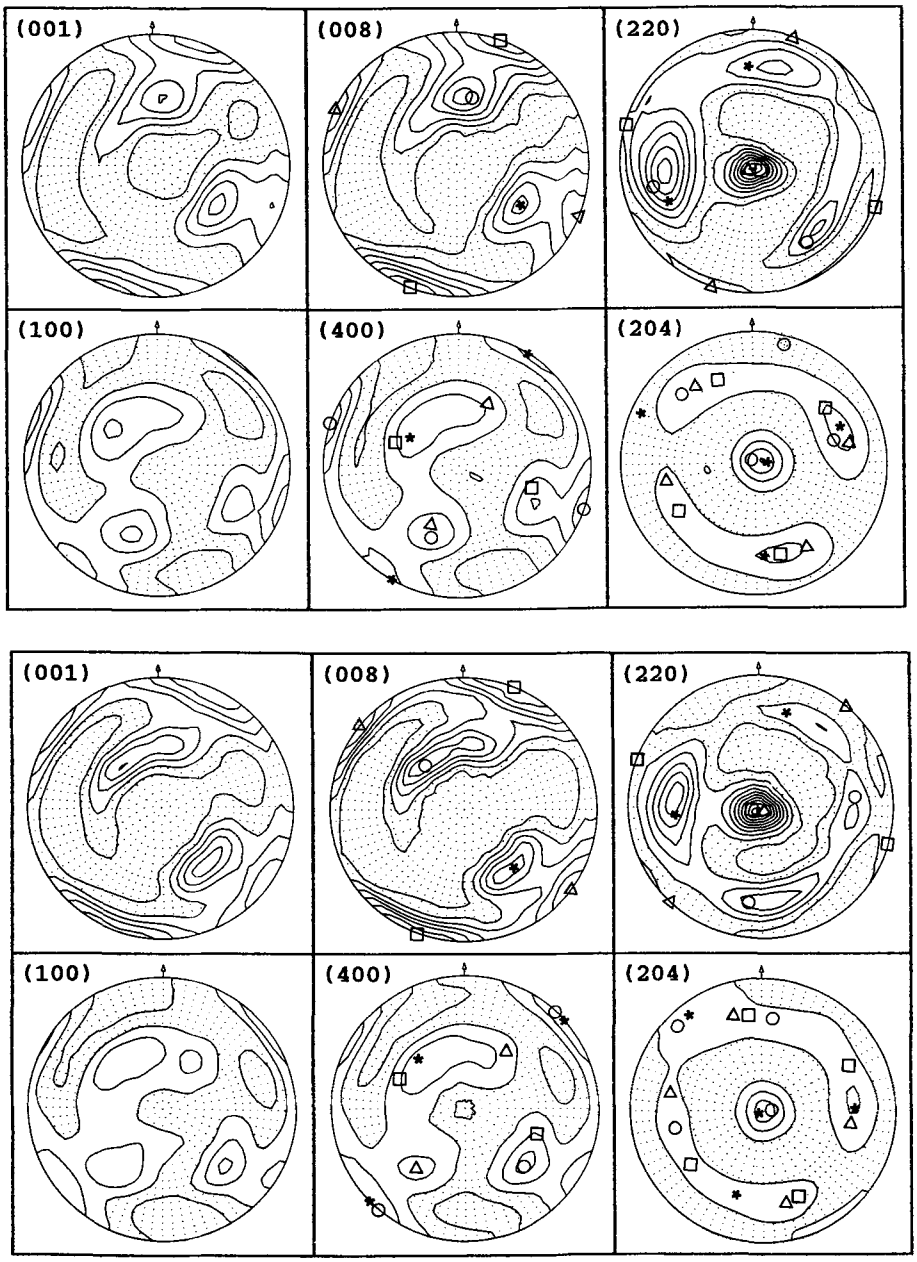

FIGS. 4 and 5. FIG. 4 (*top*). A comparison of ODF recalculated (001) and (100) pole figures with experimental (008), (400), (220) and (204) pole figures of deformed chalcopyrite showing 2 orientation components (square, triangle) with the *c*-axis perpendicular to the compression axis and 2 components (circle, star) with the *c*-axis oblique to the compression axis, sample CH8218 (25 °C, 3×10^{-5} sec^{-1}, 25%), equal area projection, dotted area: density below 1.0, contour interval 0.5. FIG. 5 (*bottom*). A comparison of ODF recalculated (001) and (100) pole figures with experimental (008), (400), (220) and (204) pole figures of deformed chalcopyrite showing 2 orientation components (square, triangle) with the *c*-axis perpendicular to the compression axis and 2 components (circle, star) with the *c*-axis oblique to the compression axis, sample CH8319 (100 °C, 3×10^{-5} sec^{-1}, 27%), equal area projection, dotted area: density below 1.0, contour interval 0.5.

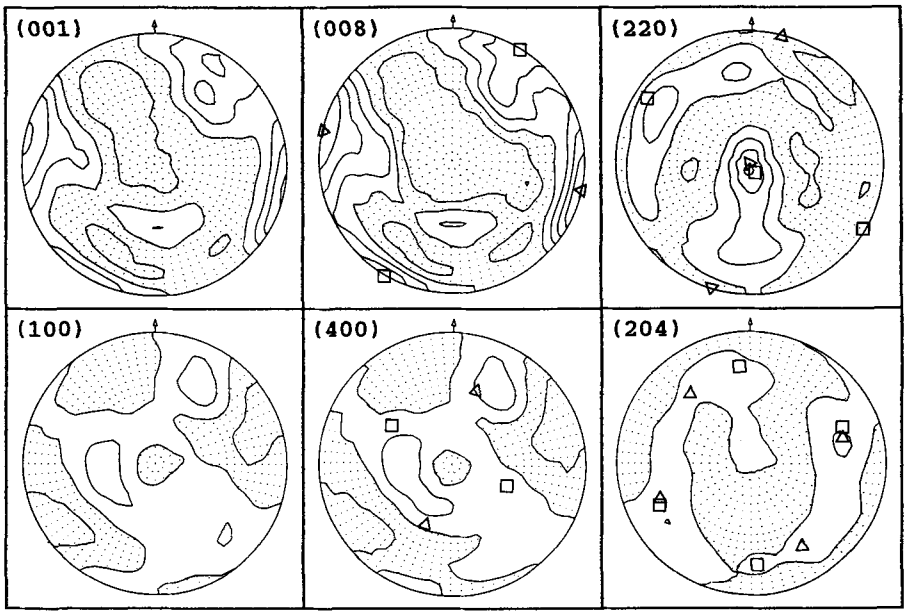

FIG. 6. A comparison of ODF recalculated (001) and (100) pole figures with experimental (008), (400), (220) and (204) pole figures of deformed chalcopyrite showing 2 orientation components (square, triangle) with the *c*-axis perpendicular to the compression axis. Sample CH8301 (200 °C, 6×10^{-6} sec^{-1}, 14%), equal area projection, dotted area: density below 1.0, contour interval 0.5.

Measured preferred orientation and interpretation

The Mt Isa ore has no pervading preferred orientation before experimental deformation. There are only local maxima at different pole positions, even within sample cylinder CH8402, for example, as shown in Fig. 1. As all experimentally deformed samples show (220/204) maxima perpendicular to the compression axis in X-ray pole figures, they are presented here in averaged density profiles to compare the fibre intensities. Relative intensities are plotted versus pole angles, that means from parallel to perpendicular to the compression axis. The examples in Fig. 2 and Fig. 3, all shortened with a strain rate of 3×10^{-5} sec^{-1}, show that the (220/204) fibre texture becomes stronger with increasing strain. The highest intensity after 10–15% shortening (Fig. 2) was found for the deformation at 200 °C, and after 25–31% shortening (Fig. 3) for the deformation at 100 °C. The fibre seems to become weaker with slower strain rate and higher temperature from 200 °C to 400 °C, but this is not shown by all samples (Jansen, 1990).

In the neutron diffraction pole figures of some of the real tetragonal reflections (Figs. 4–8) no fibre texture is visible. In order to interpret the different pole figures, which are presented here with the projection plane perpendicular to the compression axis, the (008) maxima were used to find idealised tetragonal single crystal orientations; *c*-axis poles were set into the centres of the maxima and the corresponding positions of all other reflections were calculated. The agreement of the calculated positions with the maxima of the pole figures of all reflections was the evidence for a true orientation component. The idealised poles of each crystallite orientation component are marked with a symbol (see Figs. 4–8). Similar orientation components occurring in the pole figures of different samples are marked with the same symbol. From the ODF (orientation distribution function), recalculated (001) and (100) pole figures are compared with the experimental (008) and (400) pole figures. Also given in Figs. 4–8 are the separated (220) and (204) pole figures. Specimens CH8218 and CH8319, which had been shortened by about 25% at 25 °C and 100 °C, each show a similar combination of four main orientation components (Figs. 4 and 5). There are two idealised *c*-axis orientations perpendicular to the compression axis, and two at about 40 and 50° oblique to the compression axis. The first two components contribute to a rather strong maximum of (220) perpendicular to the compression axis, whereas the two other components contribute to a weaker maximum of (204) perpendicu-

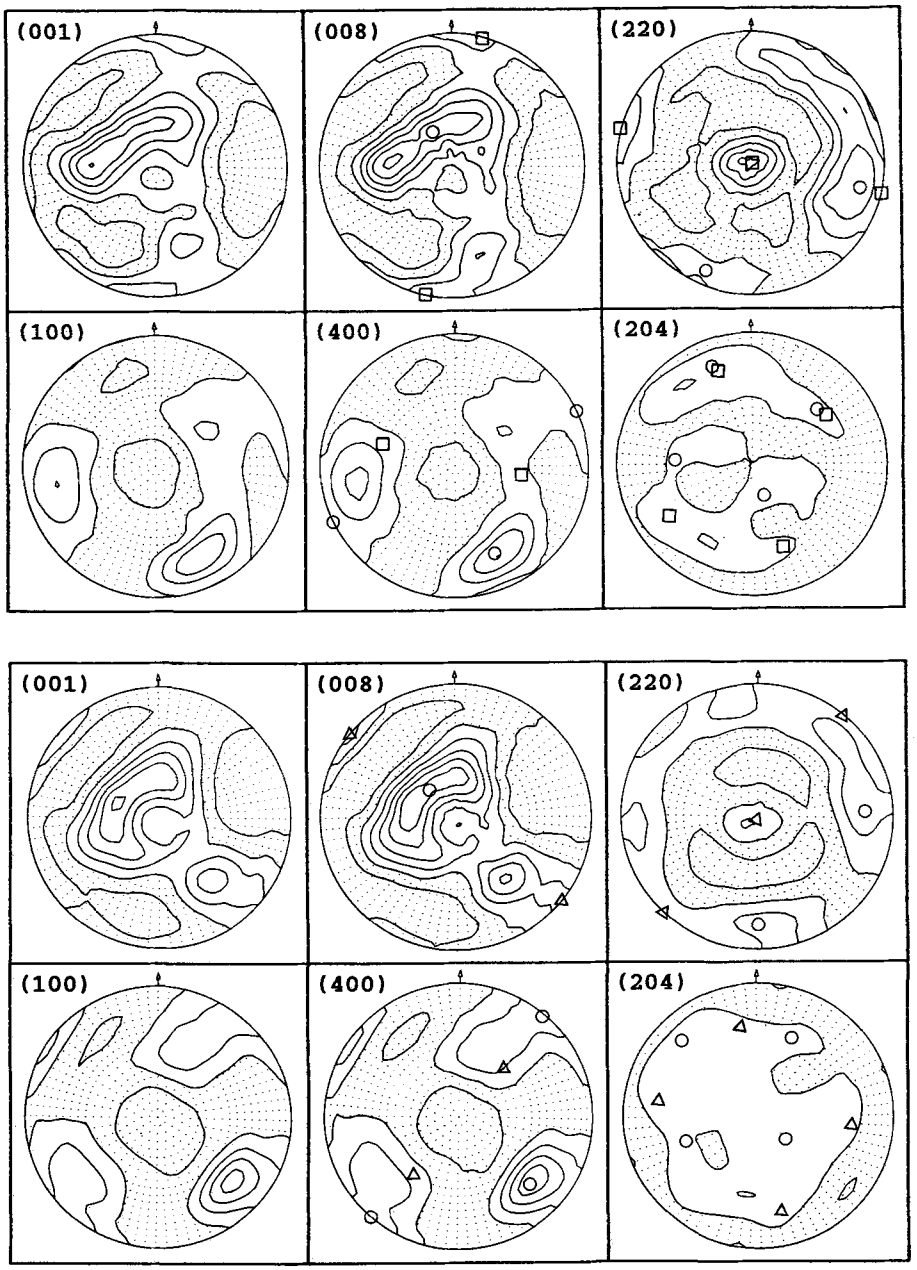

FIG. 7 and 8. FIG. 7 (*top*). A comparison of ODF recalculated (001) and (100) pole figures with experimental (008), (400), (220) and (204) pole figures of deformed chalcopyrite showing 1 orientation component (square) with the *c*-axis perpendicular to the compression axis and 1 component (circle) with the *c*-axis oblique to the compression axis. Sample CH8508 (300 °C, 3×10^{-6} sec^{-1}, 15%), equal area projection, dotted area: density below 1.0, contour interval 0.5. FIG. 8 (*bottom*). A comparison of ODF recalculated (001) and (100) pole figures with experimental (008), (400), (220) and (204) pole figures of deformed chalcopyrite showing 1 orientation component (triangle) with the *c*-axis perpendicular to the compression axis and 1 component (circle) with the *c*-axis oblique to the compression axis. Sample CH8303 (400 °C, 3×10^{-6} sec^{-1}, 15 per cent), equal area projection, dotted area: density below 1.0, contour interval 0.5.

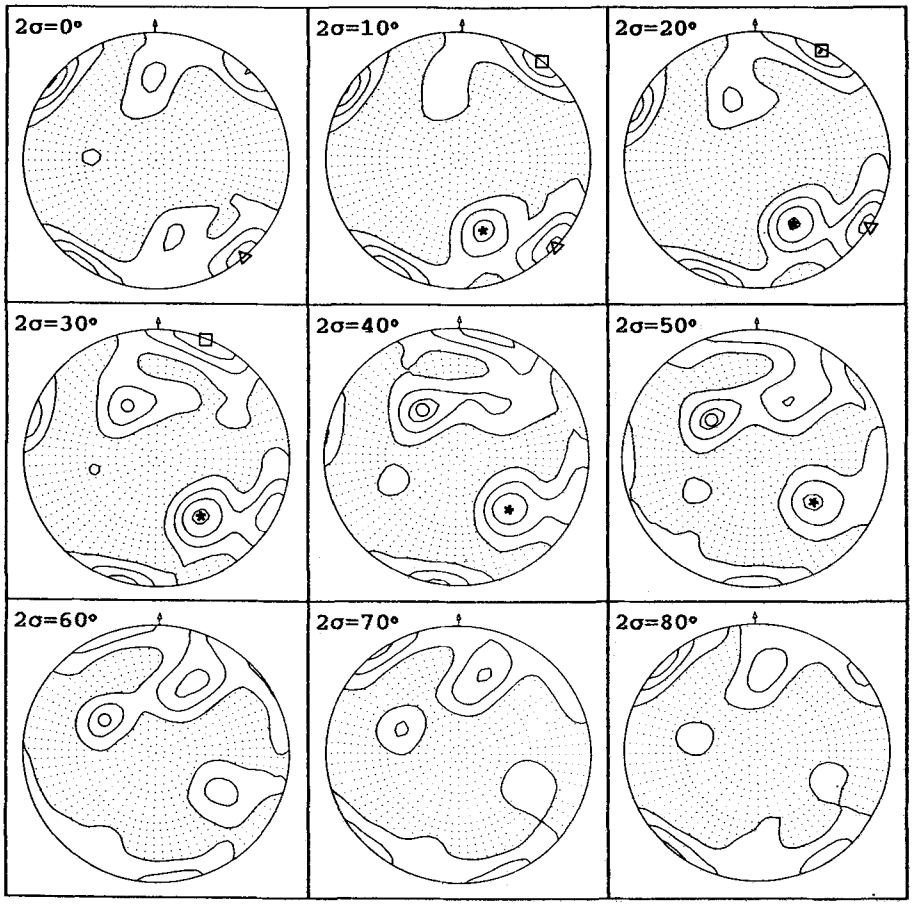

FIG. 9. Calculated ODF after 23 iterations in sigma sections $2\sigma = (\alpha + \gamma)$, with 2 orientation components (square, triangle) with the *c*-axis perpendicular to the compression axis and 2 components (circle, star) with the *c*-axis oblique to the compression axis. Sample CH8319 (100 °C, 3×10^{-6} sec^{-1}, 27%), equal projection, dotted area: density below 1.0, contour interval 0.5.

lar to the compression axis. These central maxima are of a more or less circular shape, whereas other maxima are elongated and slightly curved, probably indicating a partial fibre component. Sample CH8301, shortened about 14% at 200 °C, shows only two rather weak orientations with <001> lattice directions perpendicular to the compression axis, resulting in a weak and widely spread maximum of (220) in the centre of the projection (Fig. 6). The main crystallite orientations of samples CH8508 and CH8308, deformed at 300 and 400 °C, are characterised by two components. One component is also orientated with the *c*-axis perpendicular to the compression axis leading to (220) maxima in the centres of the pole figures (Figs. 7 and 8). The second, much stronger component with a *c*-axis maximum about 25 degrees off the centre of the projection for both of the samples, could be associated with a central maximum of (103) or (105). But this cannot be proved by the measured pole figures of these reflections because of their very low intensities and their very close position to the strong (112) and (220) reflections. They cannot be resolved reliably by means of profile analysis (Jansen *et al.*, 1992). The measured (008) and (400) and the recalculated (001) and (100) pole figures are in a very good agreement, as shown in Figs. 4 to 8.

The main texture components identified in the pole figures were verified by associated maxima in the orientation distribution functions. As examples in Figs. 9 and 10, the ODFs of samples CH8319 and CH8308 are given. The maxima in the sigma sections (Figs. 9 and 10) are marked by

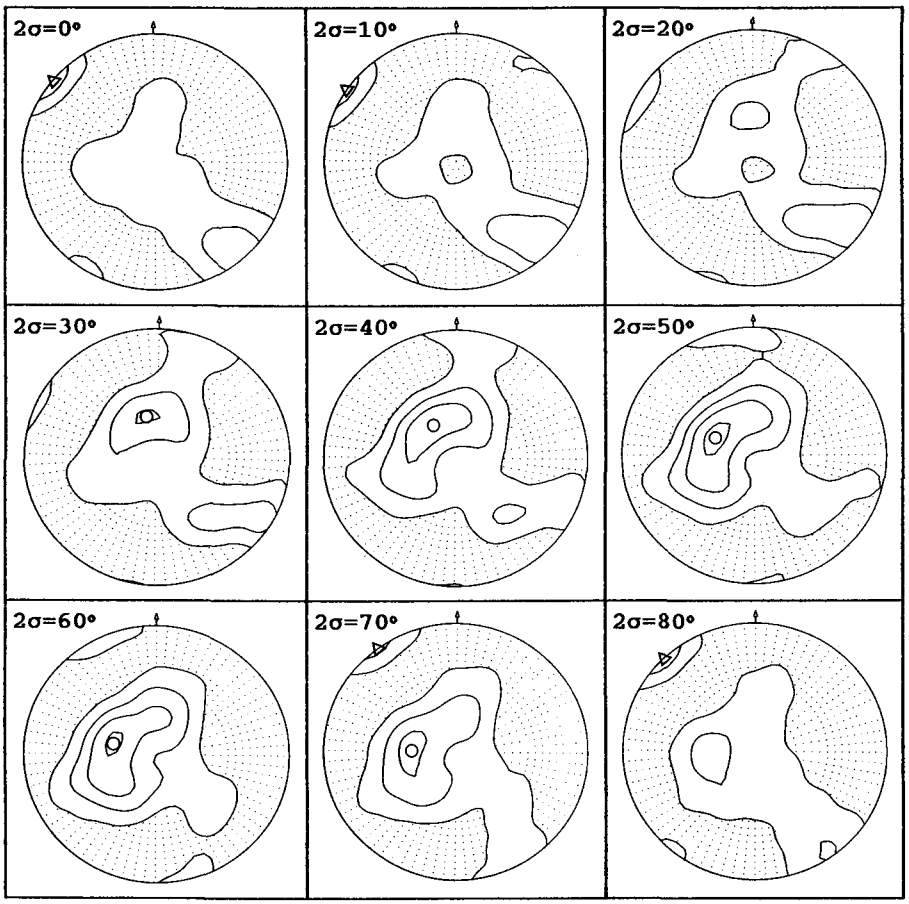

FIG. 10. Calculated ODF after 23 iterations in sigma sections $2\sigma = (\alpha + \gamma)$, with 2 orientation components (triangle) with the *c*-axis perpendicular to the compression axis and 2 components (circle) with the *c*-axis oblique to the compression axis. Sample CH8303 (400 °C, 3×10^{-6} sec^{-1}, 16%), equal projection, dotted area: density below 1.0, contour interval 0.5.

the symbols of the associated maxima in the pole figures. The elongated (001) maxima (Figs. 5 and 8) are spread over several sigma sections (Figs. 9 and 10). The analysis of the sigma sections indicates an alignment of <104> parallel to the compression axis for the second component of samples CH8508 and CH8308.

Conclusions

Neutron texture investigations provide new insights into chalcopyrite preferred orientation, not available from X-ray texture analysis. In spite of the axial symmetry of the compression experiments, no complete fibre texture has developed, neither a pseudo-cubic nor a tetragonal one. Further investigations are necessary to determine whether the different combinations of crystallite orientations are characteristic of special experimental conditions and how they depend on temperature, strain rate and total strain. Additional neutron texture measurements of one and the same sample before and after experimental deformation are intended to find out whether the local maxima in experimentally undeformed specimens prevent the development of an axial symmetry during deformation. The chalcopyrite deformation behaviour leading to a preferred orientation, seems to be different from that of other common sulfides. Naturally deformed ores from Mt Lyell, Tasmania (Cox and Etheridge, 1984) and from the Frood Mine, Sudbury, Canada (Jansen *et al.*, 1991) show a quasi single crystal preferred orientation. The latter, investi-

gated by neutron diffraction, consists of a combination of two single crystal orientations. Further neutron diffraction analyses of experimentally deformed chalcopyrite could help in the interpretation of the natural ores.

References

Atkinson, B. K. (1974) Experimental deformation of polycrystalline galena, chalcopyrite and pyrrhotite. *Inst. Mining Metallurgy Trans.*, **83**, B19–28.

Couderc, J. J. and Hennig-Michaeli, C. (1988) TEM evidence of various glide modes in experimentally strained $CuFeS_2$ crystals. *Phil. Mag.*, **A57**, 301–25.

Cox, S. F. and Etheridge, M. A. (1984) Deformation microfabric development in chalcopyrite in fault zones, Mt Lyell, Tasmania. *J. Struct. Geol.*, **6**, 167–82.

Dahms, M. (1992) The iterative series expansion method for quantitative texture analysis—Part II: Applications. *J. Appl. Cryst.*, **25**, 258–67.

—— and Bunge, H.-J. (1989*a*) A positivity method for the determination of complete orientation distribution functions. *Textures and Microstructures*, **10**, 21–35.

———— (1989*b*) The iterative series expansion method for quantitative texture analyis. I. General outline. *J. Appl. Cryst.*, **22**, 439–47.

Jansen, E. M. (1990) *Experimentelle Deformation von natürlichem, polykristallinem Chalkopyrit bei Temperaturen bis 450 °C und Verformungsten von 10^{-5} bis 10^{-8} s^{-1} unter besonderer Berücksichtigung der entstehenden Texturen.* Dissertation RWTH (Unpubl.) Aachen, 148 pp.

—— Merz, P., Siemes, H., and Will, G. (1991) Interpretation of preferred orientation in naturally and experimentally deformed chacopyrite ores by neutron diffraction texture analysis. *Textures and Microstructures*, **14–18**, 431–6 (Special Issue: Ninth Int. Conf. Text. Mat. (Icotom 9), Avignon 1990, eds. Esling, C. and Penelle, R.).

—— Merz, P., Schaeben, H., Schäfer, W., Siemes, H., and Will, G. (1992) Determination of preferred orientation of pyrite in a chalcopyrite ore by means of neutron diffraction. *Textures and Microstructures*, **19**, 203–10.

Kelly, W. C. and Clark, B.R . (1975) Sulfide deformation studies III. Experimental deformation of chalcopyrite to 2000 bars and 500 °C. *Econ. Geol.*, **70**, 431–53.

Lang, H. (1968) *Stauchversuche mit polykristallinen Kupferkiesen und deren Ergebnisse unter Berücksichtigung der Gefügeregelung.* Dissertation RWTH Aachen (Unpubl.), 131 pp.

Matthies, S., Helming, K., and Kunze, K. (1990*a*) On the representation of orientation distributions in texture analysis by σ-sections. I. General properties of σ-sections. *Phys. Stat. Sol.*, **B157**, 71–83. II.

———— (1990*b*) On the representation of orientation distributions in texture analysis by σ-sections. II. Considerations of crystal and sample symmetry, examples. Ibid., 489–507.

Mügge, O. (1920) Über Translationen am Schwefel, Periklas und Juperferkies und einfache Schiebungen am Bournonit, Pyrargyrit, Jupferglanz und Silberkupferglanz. *Neues Jahrb. Min.*, 24–54.

Roscie, W. E. (1975) Experimental deformation of natural chalcopyrite at temperatures up to 300 °C over the strain rate range 10^{-2} to 10^{-6} sec^{-1}. *Econ. Geol.*, **70**, 454–72.

Will, G., Schäfer, W., and Merz, P. (1989) Texture analysis by neutron diffraction using a linear position sensitive detector. *Textures and Microstructures*, **10**, 375–87.

[*Manuscript received 5 February 1992: revised 30 May 1992*]